frontiers in Environmental Science

ORIGINAL RESEARCH
published: 04 February 2022
doi: 10.3389/fenvs.2022.823656

Synthesis, Characterization, and Application of Ag-Biochar Composite for Sono-Adsorption of Phenol

Muhammad Naeem Khan[1], Maria Siddique[1], Nosheen Mirza[2], Romana Khan[1], Muhammad Bilal[1], Nadia Riaz[1], Ummara Waheed[3], Irum Shahzadi[4], Asmat Ali[5], Magda H. Abdellattif[6], Gaber El-Saber Batiha[7], Ahmed Al-Harrasi[8]* and Ajmal Khan[8]**

[1]Department of Environmental Sciences, COMSATS University Islamabad, Abbottabad Campus, Abbottabad, Pakistan, [2]Department of Soil and Environmental Sciences, Ghazi University, Dera Ghazi Khan, Pakistan, [3]Institute of Plant Breeding and Biotechnology, Muhammad Nawaz Shareef University of Agriculture Multan, Multan, Pakistan, [4]Department of Biotechnology, COMSATS University Islamabad, Abbottabad Campus, Abbottabad, Pakistan, [5]Department of Environmental Sciences and Engineering, School of Environmental Studies, China University of Geosciences, Wuhan, China, [6]Department of Chemistry, College of Science, Taif University, Taif, Saudi Arabia, [7]Department of Pharmacology and Therapeutics, Faculty of Veterinary Medicine, Damanhour University, Damanhour, Egypt, [8]Natural and Medical Sciences Research Center, University of Nizwa, Nizwa, Oman

OPEN ACCESS

Edited by:
Gbekeloluwa B. Oguntimein, Morgan State University, United States

Reviewed by:
Joshua O. Ighalo, Nnamdi Azikiwe University, Nigeria
Mohamed Hassaan, National Institute of Oceanography and Fisheries (NIOF), Egypt

***Correspondence:**
Maria Siddique
maria@cuiatd.edu.pk
Ahmed Al-Harrasi
aharrasi@unizwa.edu.om
Ajmal Khan
ajmalkhan@unizwa.edu.om

Specialty section:
This article was submitted to Water and Wastewater Management, a section of the journal Frontiers in Environmental Science

Received: 27 November 2021
Accepted: 10 January 2022
Published: 04 February 2022

Citation:
Khan MN, Siddique M, Mirza N, Khan R, Bilal M, Riaz N, Waheed U, Shahzadi I, Ali A, Abdellattif MH, El-Saber Batiha G, Al-Harrasi A and Khan A (2022) Synthesis, Characterization, and Application of Ag-Biochar Composite for Sono-Adsorption of Phenol. Front. Environ. Sci. 10:823656. doi: 10.3389/fenvs.2022.823656

The silver-embedded wheat straw biochar (Ag–WBC) composite was tailored effectively via the green synthetic route and was used as a nano-adsorbent for the removal of phenol by using adsorption and sono-adsorption processes. *Ligustrum lucidum* leaf extract was employed as a reducer to prepare silver nanoparticles, and biochar was synthesized from wheat straw via pyrolysis at 450–500°C. The synthesized biochar and Ag–WBC were characterized by using UV–Vis, SEM, EDX, and FTIR. The study confirms the ability of plant leaf extract of *L. lucidum* to synthesize AgNPs and Ag–WBC composites for the first time. UV–vis spectroscopic analysis confirms the formation of AgNPs and Ag–WBC composites (400–440 nm). SEM results showed that the size of the Ag–WBC composite is in the range of 80–100 nm. The elemental profile of the synthesized Ag–WBC composite shows a higher count at 3 kev due to silver. FTIR analysis revealed the presence of various functional groups involved in reducing Ag metal ions into Ag nanoparticles onto the surface of the composite. Batch experiments executed adsorption and sono-adsorption studies on WBC and Ag–WBC composites, and the results revealed that under optimum conditions, that is, pH= 3, adsorbate concentration= 10 mg L^{-1}, adsorbents dosage= 0.05 g, time= 90 min, and US power = 80 W, the phenol removal efficiencies onto Ag–WBC composite were 78% using sono-adsorption compared to the non-sonicated adsorption. Langmuir and Freundlich isotherm models for fitting the experimental equilibrium data were studied, and the Langmuir model was chosen as an efficient model for the sono-adsorption process. The feasibility of the sono-adsorption process was also evaluated by calculating kinetics.

Keywords: green synthesis, Ag–biochar/composite, sono-adsorption, phenol, wastewater treatment

INTRODUCTION

Pollution from toxic contaminants is a significant concern among environmental issues of the 21st century due to various industrial activities and rapid development (Auwal et al., 2018; Rene et al., 2018; Kumar et al., 2021). Being an important raw material, phenol has been used for many industrial and non-industrial purposes (Mohammed et al., 2018; Kalogianni et al., 2020). It is water-soluble, acidic, and easily mixes from different sources, such as petroleum refinery, textile, paint, pulp, medicine, leather, dye, pesticide, and pharmaceutical industries, into wastewater (Ali et al., 2018; Younis et al., 2020; Hamad, 2021). Phenolic compounds are categorized as one of the most hazardous compounds in the environment (Hejazi et al., 2019; Mojoudi et al., 2019; Pantić et al., 2021), and phenol is chosen as the model pollutant in this study because it has been listed as a priority pollutant due to its toxicity and hard biodegradability once it is discharged into the natural environment. The high toxicity and low biodegradability of phenol pose a severe threat to the environment, even in low concentrations (Alnasrawy et al., 2021). Phenol and its derivative compounds may cause blindness, liver and pancreas damage, kidney failure, dark urine, paralysis, nervous disorder, and cancer (Parada Jr et al., 2019; Thang et al., 2019). According to the international regulatory agencies of the World Health Organization and EPA, the estimated value of phenol >1 ppm is carcinogenic and non-acceptable in water resources for inhabitants (Zarin et al., 2018). Due to its wide use and hazardous consequences, the removal of phenol from wastewater attains considerable interest among researchers by different conventional and advanced methods, that is, including adsorption/biosorption (Francis et al., 2020), biological degradation (Tomei et al., 2021), electrochemical oxidation (Yavuz and Koparal, 2006), solvent extraction (Liu et al., 2013), membrane filtration (Li et al., 2010), and photocatalytic degradation (Mohamed et al., 2020).

Adsorption has been a topic of interest among researchers due to its high efficiency, cost-effectiveness, lower operating cost, and simple operating process (Villegas et al., 2016; Mohammed et al., 2018). Exploring new adsorbent materials to enhance the removal efficiency of pollutants has always been an imperative issue in adsorption. In literature, different carbon-rich materials have been investigated for the removal of phenolic contaminants from wastewater (Yadav et al., 2019).

Biochar has vast applications and gains excessive focus for eradicating organic pollutants (Premarathna et al., 2019). Using the pyrolysis method under limited oxygen conditions, it can be produced from various agricultural wastes such as woodchips, wheat straws, shells, bagasse, and cow manure (Nanda et al., 2016). However, raw biochar has certain limitations due to pore volume and weak functional groups, restricting its practical use. Therefore, to achieve better performance and enhanced adsorption capacity, techniques like fabrication of metal/metal oxides, surface functionalization, and magnetic induction have been used to modify biochar (Peng et al., 2019; Liu et al., 2020). The modified biochar with metal ions shows better adsorption efficacy than activated carbon (Yin et al., 2018).

Metallic nanoparticles have been synthesized by various physical, chemical, and biological methods and are extensively being used in numerous fields. The use of eco-friendly synthesis for nanoparticles (NPs) is termed green synthesis, and it is preferred because it is a single step process. This cost-effective and eco-friendly method does not require high pressure, temperature, energy, and toxic chemicals (Khan et al., 2021). The size of nanoparticles ranges from 1 to 100 nm and is composed of control-fabricated material. Among metallic nanoparticles, silver nanoparticles (AgNPs) are critical due to their unique properties, such as good electrical conductivity, photo-electrochemical activity, and strong reduction power. Many researchers have reported plants, bacteria, fungi, and enzymes for synthesizing AgNPs (Mariselvam et al., 2014) and their wide application. A plant extract (leaf, root, stem, bark, fruit, bud, and latex) produces efficient capping material to stabilize AgNPs (Ahmed et al., 2016). A variety of plants have been reported to synthesize silver metal (Ag^o) nanoparticles from silver ions (Ag^+). Plants such as *Allium cepa* (Sharma et al., 2018), *Thymbra spicata* (Veisi et al., 2018), and *Azadirachta indica* (Saad et al., 2017) had been utilized for the synthesis of AgNPs and their application in pollutants removal. *Ligustrum lucidum* (also known as Chinese privet) is a flowering plant that belongs to the olive family Oleaceae. It is native to the southern half of China and widely distributed in tropical and subtropical regions. The bioactive components of *Ligustrum lucidum* fruits are triterpenes, secoiridoid glucosides, volatile components, flavonoids, and phenolic compounds that have various pharmacological effects in the field of nanomedicines (Saad et al., 2017).

Moreover, in recent years, coupling ultrasound irradiation with the adsorption process has received imperative attention (Arefi-Oskoui et al., 2019). The efficacy of the adsorption process can be further improved by applying ultrasonication (Hamza et al., 2018). An ultrasonic phenomenon can be used for the acceleration of chemical reactions and mass transfer because of acoustic cavitation (formation, growth, and collapse of bubbles in liquid) and formation of new adsorbent sites on adsorbent (Parthasarathy et al., 2016; Wang et al., 2017) and also creates numerous micro-cracks on the upper layer of the adsorbing material which increases the surface area between the adsorbent and adsorbate (Cuerda-Correa et al., 2020). Furthermore, the sono-adsorption process is found to be efficient in controlling the concentration of pollutants. It is economically viable and the best alternative to conventional methods in terms of chemical utilization and environmental impacts (Ali et al., 2018).

The present study aims to synthesize biochar from wheat straw, and silver (Ag)-embedded engineered biochar using a novel, effortless, low-cost, and green approach to remove phenol using adsorption and sono-adsorption processes. To the best of our knowledge, the application of Ag-loaded wheat straw biochar for adsorptive uptake of phenol is unexplored. The effect of different operating parameters for the removal phenol under variable operating conditions was investigated using adsorption and

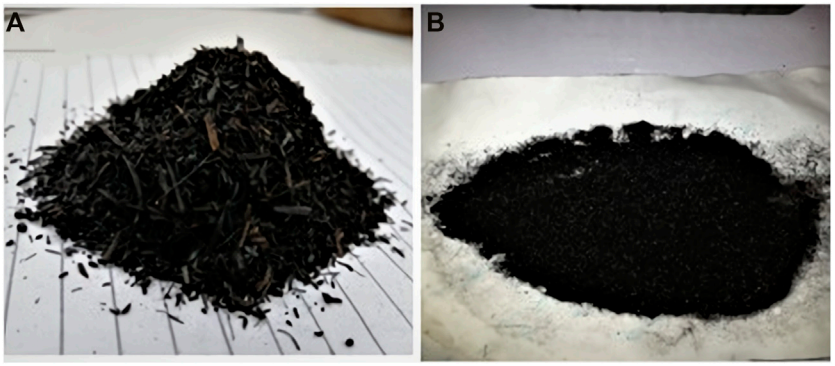

FIGURE 1 | Wheat Straw Biochar **(A)** as-synthesized **(B)** washed with distilled water.

sono-adsorption. Furthermore, the characterization study of wheat straw biochar and Ag–WBC nanocomposites was examined using UV–vis spectrophotometry, scanning electron microscopy, energy-dispersive X-ray spectrometry, and Fourier-transformed infrared spectroscopy.

MATERIALS AND METHODS

Phenol C_6H_5OH (CAS No. 108-95-2) was acquired from Sigma-Aldrich. Methanol (CH_3OH), hydrochloric acid (HCl), sodium hydroxide (NaOH), and silver nitrate (Ag-$NO_3.2H_2O$) were purchased from Merck (Germany). Analytical grade chemicals were used for the experiments without further purification.

Synthesis of Biochar From Wheat Straw

Wheat straw was collected from Chakli Padroi Darband, Khyber Pakhtunkhwa, in the mowing season. The wheat straw was washed, dried, ground, and sieved to particles of 0.5-mm mesh at room temperature. Consequently, the material was pyrolyzed in a muffle furnace under a continuous nitrogen flow for 2 h at 450–500°C. The resulting biochar was repeatedly washed with distilled water until neutral pH and dried at 45°C for 12 h as shown in (**Figure 1**). The obtained biochar was secured in zipper bags for further use (Zhang et al., 2019).

Plant Material Collection

Ligustrum lucidum was collected from COMSATS University Islamabad Abbottabad Campus, Pakistan. The plants were washed, kept in the shade for drying, and then grounded to powder. A grounded plant of 25 g was mixed at a ratio of 4:1 in 300 ml of methanol and distilled water. Ultrasonic-assisted extraction was performed for 1 h at US power 80 W at a temperature of 30–35°C. An ultrasonic bath (Cleaner model U Tech Products, Inc., NY, United States) was used for ultrasound-assisted extraction studies (35 kHz). The ultrasonic bath was calibrated by using the calorimetric method (Siddique et al., 2014; Ali et al., 2018). Rotary evaporation was performed after filtration to get the plant crude extract, and then the solution was kept over for more evaporation (Zia et al., 2017).

Synthesis of Silver Nanoparticles

A stock solution of $AgNO_3$ (1 Molar) was prepared by adding 1.7 g of silver nitrate with a total volume of 10 ml in distilled water. The various concentrations were further prepared by dilution methods such as 1 mM, 5 mM, and 10 mM. For this, 0.25 ml of silver nitrate was taken from the stock solution and filled up to the desired volume of 49.75 ml distilled water.Meanwhile, 250 mg of plant crude extract was mixed in 50 ml methanol. Both the solutions were combined to form a 100 ml solution followed by incubation at 37°C for 24 h. UV–vis spectrophotometry was conducted to observe the synthesis of silver nanoparticles at 0 min and after 24 h. The color change of the solution from light brown to dark brown confirmed the formation of silver nanoparticles. The intensity of color increased, which confirmed the reduction of Ag ions and the formation of silver nanoparticles. Moreover, the samples were centrifuged at 10,000 rpm for 15 min at 20°C. The supernatant was discarded, and the pellets of nanoparticles were then washed twice with distilled water using a centrifuge machine and dried for further use (Chandran et al., 2006; Zia et al., 2017).

Synthesis of Silver Biochar Composite

Ag–WBC was synthesized through a modified procedure described elsewhere (Kaushal et al., 2019; Santhosh et al., 2020; Wang et al., 2020). In this method, 0.1 g of biochar was mixed in 5 mM prepared silver nitrate solution (50 ml) and stirred for 30 min. Then, 250 mg of prepared extract of *Ligustrum lucidum* leaves were mixed in 50 ml of methanol followed by stirring. Both prepared solutions (100 ml) were mixed followed by ultrasonication for 30 min at 80 W US power. After this, the mixture was incubated at 37°C for 24 h. The color change of the solution confirmed the formation of silver biochar composites. Furthermore, this solution was centrifuged at 10,000 rpm for 15 min. The resultant precipitates were filtered, followed by washing with distilled water, and dried at 70–80°C for 12 h. The Ag–WBC composite thus obtained was annealed at 300°C for 1 h and stored for practical use (**Figure 1**).

Preparation of Phenol Solution

A stock solution of 500 mg L^{-1} of phenol was prepared. From the stock solution, different concentrations of phenol standards 1, 5, 10, 25, 50, and 100 mg L^{-1} were ready for experimentation purposes. The pH was adjusted using dilute HCl and NaOH (1 M), respectively.

Screening and Optimization Studies

Biochar and Ag–WBC were screened for their adsorption capacity of phenol against various operational parameters, including contact time (0–120 min), adsorbent dosage (0.025–0.1 g) pH (3–9), and initial phenol concentrations of (5–100 mg L^{-1}). For a typical batch experiment, an adsorbent dose of 0.05 g L^{-1} was used with a total of 100 ml of reaction volume at pH 3. The solution was stirred using a magnetic stirrer for 2 h at 500–600 rpm. The optimum conditions for adsorption were found as phenol conc. = 10 mg L^{-1}, pH = 3, time = 90 min, adsorbent dosage = 0.05 g L^{-1}, and operating room temperature. Sono-adsorption experiments were carried out in a digital ultrasonic bath (Cleaner model U Tech Products, Inc., NY, United States). All the similar conditions were as of the adsorption process. The best selected after the screening of adsorption was further evaluated for sono-adsorption against reaction parameters such as pH, adsorbent dosage amount, and impact of phenol concentration. The parameters of the ultrasonic bath were set at a time of 120 min, US power of 80 W, temp 30–35°C, and frequency of 35 kHz as reported in our previous study (Ali et al., 2018). The pH of the phenol solution was adjusted by adding HCl and NaOH using a pH meter (JENCO 6175). Samples were collected at regular intervals for the effect of contact time, and a final concentration of phenol was determined by a UV–vis spectrophotometer at 270 nm. Samples were centrifuged at 5,000 rpm for 5 min followed by filtration. The amount of phenol adsorbed by as-prepared Ag–WBC was determined by the equation:

$$\text{Phenol removal}\,(\%) = \frac{Ci - Cf}{Ci} * 100, \tag{1}$$

where C_i = Initial concentration of phenol before adsorption and sono-adsorption and C_f = Final concentration of phenol after adsorption and sono-adsorption.

Characterization of Biochar and Silver-Embedded Wheat Straw Biochar

Synthesized biochar and Ag–WBC were characterized to study their physicochemical properties. A UV–vis spectrum of the aqueous medium was used to confirm Ag nanoparticles, and Ag–WBC composites showed absorption peak in the range of 400–480 nm with a double-beam UV–vis spectrophotometer (T80 + PG Instruments, United Kingdom). Adsorptive performance was determined at a wavelength of 270 nm for phenol removal. Surface morphology (using scanning electron microscopy, SEM) was examined by taking micrographs at various resolutions with the JSM-5910 scanning electron microscope (JEOL, Tokyo, Japan) at the Central Resource Laboratory (CRL), Peshawar. Energy-dispersive X-ray (EDX) analysis was used to analyze the presence of elemental silver. The surface interaction of biochar and Ag–WBC was analyzed by Fourier-transformed infrared spectroscopy (FTIR) in the range of 400 per cm to 4,000 per cm.

Adsorption Isotherms

Adsorption isotherms were used to determine the interaction between the adsorbent and adsorbate. The entire transfer process took place until the equilibrium was established between the two phases. These isotherms were used to evaluate adsorption phenomena, contaminant adsorption strength, and the practical design of the adsorption process (Chung et al., 2015). This study used two isotherms to evaluate experimental data, that is, the Langmuir and Freundlich isotherms. The Langmuir isotherm describes the concept of a single adsorbate in a single molecular layer. The model in this study is expressed as

$$\frac{1}{q_e} = \frac{1}{q_{max}} + \left(\frac{1}{q_{max} K_{ads}}\right) \frac{1}{C_e}, \tag{2}$$

where Q_e represents the amount of phenol adsorbed (mg g^{-1}), C_e represents equilibrium concentration (mg L^{-1}), K_{ads} represents the equilibrium adsorption constant (mg L^{-1}), and $Q_m = Q_e$ for complete monolayer adsorption capacity (mg g^{-1}). R_L is a dimensionless constant (separation factor) that was measured for best-fit.

Langmuir and is generally expressed as

$$R_L = \frac{1}{1 + (q_{max} \times b) C_0}. \tag{3}$$

The value of R_L indicates the isotherm shape to be linear (R_L = 1), favorable (0 < R_L < 1), unfavorable (R_L > 1), and irreversible adsorption (R_L = 0). The Freundlich isotherm is used to model multilayer adsorption on heterogeneous surfaces adsorption. Heterogeneity was due to different functional groups on the surface and the numerous adsorbent–adsorbate interactions. Mathematically, this model is used as

$$q_e = K_f C_e 1/n, \tag{4}$$

where K_f is the Freundlich isotherm constant, C_e and q_e indicate the residual phenol in the aqueous phase, and phenol adsorbed by Ag–WBC, and n represents the heterogeneity of the adsorbent.

Adsorption Kinetics

In this study pseudo-first- and pseudo-second-order kinetics (linear form) is applied on the ultrasonic-adsorptive data. To check the effect of contact time (10–90 min) on adsorption, an initial concentration of 10 mg L^{-1} of phenol was prepared (100 ml). An adsorbent dose of (0.05 g L^{-1}) was added to the phenol solution and was stirred for 2 h at 500–600 rpm. At various time intervals, the sample was taken and analyzed for phenol concentration. The amount of phenol adsorbed at different time intervals was calculated by employing the following formula:

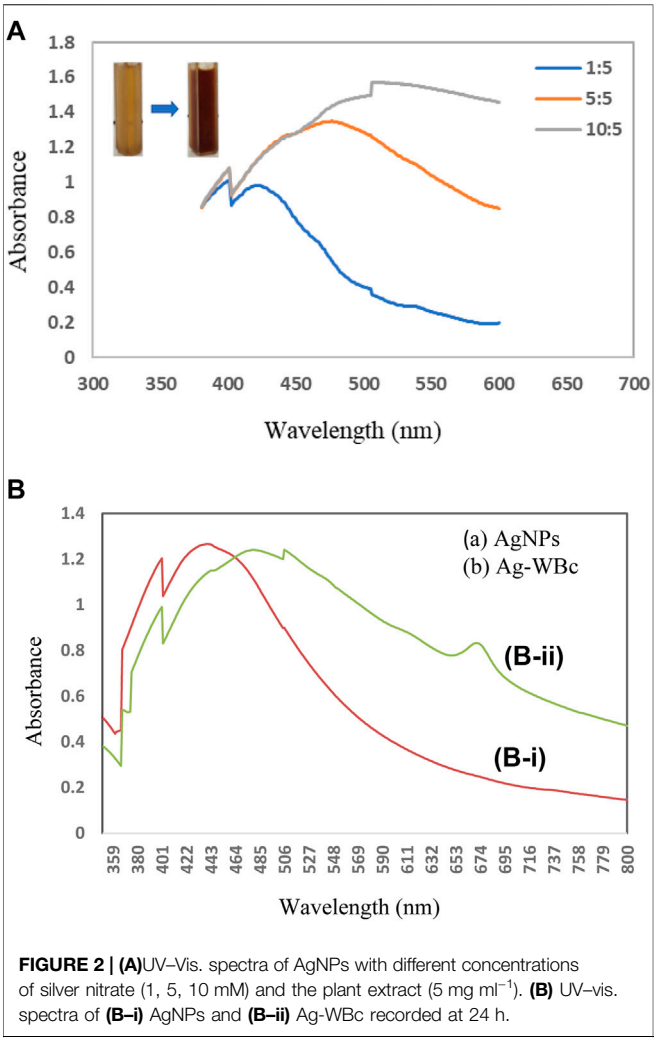

FIGURE 2 | (A)UV–Vis. spectra of AgNPs with different concentrations of silver nitrate (1, 5, 10 mM) and the plant extract (5 mg ml^{-1}). **(B)** UV–vis. spectra of **(B–i)** AgNPs and **(B–ii)** Ag-WBc recorded at 24 h.

$$Q_t = \frac{(Q_o - Q_t)}{W} X\, V, \tag{5}$$

where Q_t is the amount of phenol adsorbed in time t, and Q_o and Q_t are initial and equilibrium concentrations, respectively. The volume of phenol solution taken is represented by V (L) and is the amount of adsorbent in g.

Pseudo-First-Order Kinetics

To calculate pseudo-first-order kinetics for the sono-adsorption system, the following equations were used:

$$\ln(Q_e - Q_t) = \ln(Q_e) - k_1 t, \tag{6}$$

where Q_t is the amount adsorbed at time t, Q_e is the equilibrium amount, it is time in minutes, and K_1 is the rate constant.

Pseudo-Second-Order Kinetics

For pseudo-second-order kinetics, the following equation was applied:

$$\frac{t}{Q_t} = \frac{1}{k_2 Q_e^2} + \left(\frac{1}{Q_e}\right) t. \tag{7}$$

RESULTS

Biosynthesis and Characterization of Adsorbents

Color Change and UV–vis Spectroscopic Profile of Synthesized AgNPs and Silver-Embedded Wheat Straw Biochar

The present study focused on developing silver nanoparticles (AgNPs), and silver-embedded biochar composites (Ag–WBC) using an environment-friendly, cost-effective, and green approach using *L. lucidum* plant leaf extract as a reducing agent. For the synthesis of silver nanoparticles, *L. lucidum* plant leaf extracts (5 mg ml^{-1}) and variable concentrations of silver nitrate (1, 5, 10 mM) were used (**Figure 2A**). Meanwhile, for the synthesis of silver biochar composites (Ag–WBC), 0.1 g of biochar was added with optimum concentration of the plant extract and silver nitrate solution. An apparent change in the color of the reaction mixtures was noticed from light brown to dark brown after 24 h of incubation at room temperature (**Figure 2A**). The color change indicates the reduction of silver ions (Li et al., 2019) to AgNPs and Ag–WBC formation. The formation of AgNPs and Ag–WBC was further confirmed by UV–vis spectral analysis, which was measured at the wavelength ranging from 350 to 800 nm after 24 h of incubation. It can be observed from **Figure 2B** that the UV–vis spectrum of reaction mixtures recorded at 24 h showed a peak of AgNPs at λ_{max} = 439 nm and Ag–WBC at λ_{max} = 470 nm. The peaks at λ_{max}= 439 and 470 nm are due to nanoparticles and composites' surface plasmon resonance (SPR) (El-Naggar et al., 2017). The SPR value was higher in composites than that obtained in the case of AgNPs. It was observed that the SPR band shifted from shorter to longer wavelengths (Femila et al., 2014; Ashraf et al., 2016) The SPR band arose due to the collective oscillations of the conduction electrons of nanoparticles and composites in the presence of visible light which is highly influenced by the shape and size of the nanoparticles and composites. The ratio of *L. lucidum* plant extract and silver nitrate plays a vital role in the synthesis of NPs. The cluster of nanoparticles is highly reliant upon the biomolecules that are present in the plant extract. This biomolecule plays an essential role in reduction, stabilization, and as a restricting agent to protect nanoparticles from aggregation. It is observed that the equal ratio of plant extract and silver nitrate dramatically affects the number of biomolecules which reduces the metal, and thereby more deep coloring of the reaction mixture takes place (Amina and Guo, 2020; Restrepo and Villa, 2021).

Scanning Electron Microscopy and Energy-dispersive X-Ray

Scanning electron microscopy (SEM) is one of the most important tools for describing the surface morphology of adsorbents. SEM images of WBC and Ag–WBC composites were used to study the surface morphology. The results displayed that the WBC having no crystalline structure is mainly limited to uniform-sized particles agglomerated together and producing large irregular clusters

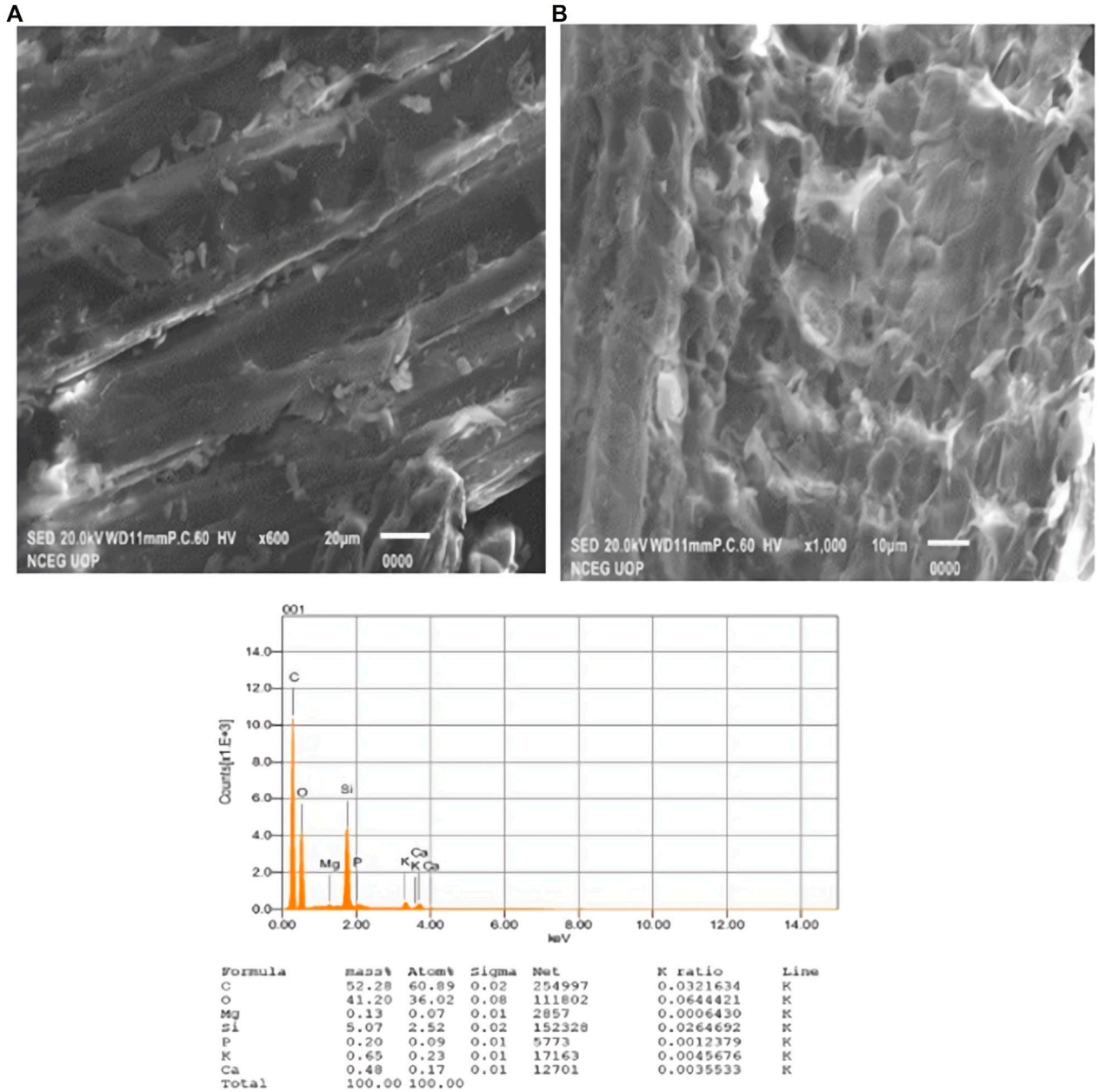

FIGURE 3 | (A) SEM images and EDX spectra of biochar prepared from wheat straw. **(B)** SEM images and EDX spectra of Ag–Biochar composites.

(**Figure 3A**). The EDX spectrum of WBC describes the elemental analysis of the material where no Ag peaks are seen. SEM images of synthesized Ag–WBC were found to show the spherical morphology of Ag nanoparticles with an average size of 80–100 nm on the surface of WBC (**Figure 3B**). The EDX spectrum of synthesized Ag–WBC confirms the fact that the composite not only has higher amounts of elemental carbon and oxygen, but it also contains significant quantities of ash elements such as Al, Si, Cl, and Ag as reported in previous studies (Nebojsa et al., 2012; Li et al., 2017; Kaushal et al., 2019; Singh et al., 2020). Some of these elements were originated from the biomolecules present in *L. lucidum* leaf extracts that were bound to the surface of AgNPs. The results were almost similar to the previous literature (Kaushal et al., 2019; Singh et al., 2020).

Fourier-Transformed Infrared Spectroscopy

FTIR spectroscopy was performed to comprehend the surface chemistry of WBC and Ag–WBC. The FTIR spectra of the samples are displayed in **Figure 4**, respectively. The WBC spectrum shows absorption bands at 3,200–3,800 cm^{-1}, 2,920.54 cm^{-1}, 1,575.70 cm^{-1}, 1,514.42 cm^{-1}, 1,027.98 cm^{-1},

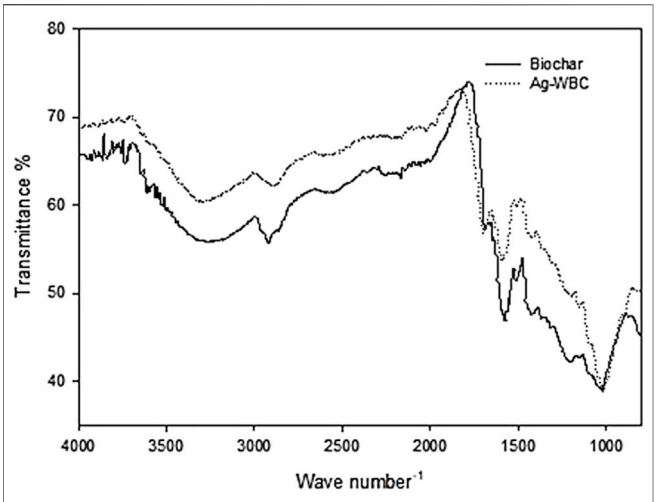

FIGURE 4 | FTIR spectra of Biochar (WBC) and Ag–Biochar composites (Ag–WBC).

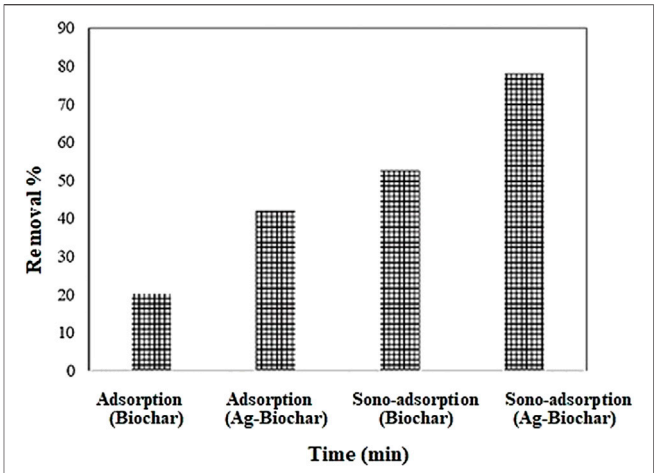

FIGURE 5 | Adsorption and sono-adsorption of phenol at different conditions (Experimental conditions: phenol conc. = 10 mg L^{-1}, adsorbent dose = 0.05 g, pH = 3, ultrasound frequency= 35 kHz, US power= 80 W).

and the spectrum of Ag–WBC showed the bands at 3,270.48 cm^{-1}, 2,883.88 cm^{-1}, 1,697.52 cm^{-1}, 1,590.73 cm^{-1}, and 1,023.37 cm^{-1}, respectively. The absorbance between 3,200 and 3,800 cm^{-1} showed cellulosic O–H stretching characteristic of –OH groups in the WBC and significantly decreased in Ag–WBC composites. The O–H stretching mode of hexagonal groups and adsorbed water can be assigned to this band (Saleh et al., 2013). Bands obtained at 2,920.54 cm^{-1} and 2,883.88 cm^{-1} correspond to aliphatic C–H–stretching vibrations, indicating original organic residues such as polymeric (cellulose, hemicellulose, and lignin) and fatty acids. The C=C stretching of the aromatic and asymmetric bending of the C–H group was due to the bands 1,575.70 cm^{-1}, 1,697.52 cm^{-1}, 1,514.42 cm^{-1}, and 1,590.73 cm^{-1}which agreed with the study by Biswas et al. (2017). The bands at 1,027.98 cm^{-1} and 1,023.37 cm^{-1} were due to the vibration of C–O stretching of polysaccharides and the presence and intensities of these peaks (Zhou et al., 2016).

Screening and Optimization Studies

At different operational conditions, the phenol adsorption and sono-adsorption efficiency using wheat straw biochar (WBC) and silver-biochar composite (Ag–WBC) were analyzed. It can be shown in **Figure 5** that the screening and optimization techniques were found in increasing order: sono-adsorption Ag–WBC > sono-adsorption WBC > adsorption Ag–WBC > adsorption WBC with the percentage removal contribution 78%, 52.3%, 42.1%, and 19.8%, respectively. However, in the presence of ultrasonic-assisted adsorption with Ag–WBC, the phenol removal was 78% in 90 min of contact time. The results confirmed that the sequestration was enhanced under sono-adsorption as compared to the traditional adsorption process. Ultrasound revealed the physical and chemical effects through the phenomenon of cavitation. The principal chemical effect of cavitation was the generation of highly reactive radicals. In contrast, the principal physical effect is the generation of strong convection in the system by three mechanisms, namely,

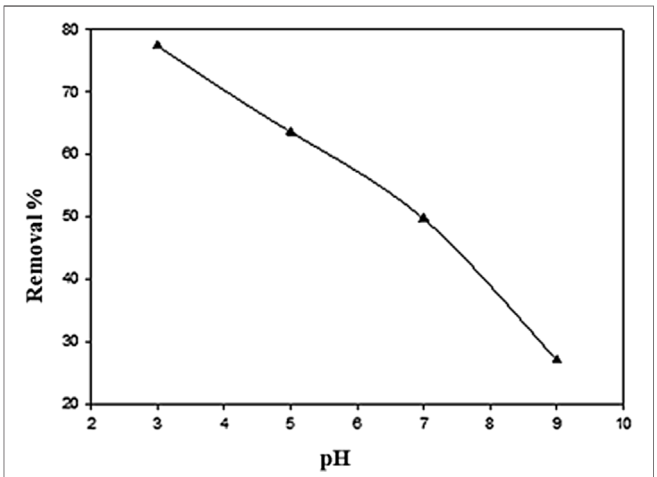

FIGURE 6 | Effect of pH on percentage removal of phenol using Ag–WBC by sono-adsorption (Experimental conditions: phenol conc. = 10 mg L^{-1}, contact time = 90 min, adsorbent dose = 0.05 g, ultrasound frequency = 35 kHz, US power= 80 W).

microturbulence (or micro-convection), sound (or shock) waves, and microjets. Due to micro-bubbles' extreme temperature and pressure conditions, there was a generation of free radicals due to the dissociation of entrapped vapor molecules. At the disintegration of the bubble at the point of maximum compression, these radicals were released into the medium, which resulted in the activation of available reactive sites on accumulated particles surface, releasing enough kinetic energy to drive reactions to completion where they induced and accelerated chemical reactions, well-known as sonochemical reactions (Bansode and Rathod, 2017), which enhanced the removal percentage of phenol by boosting the attraction between competing species (Kaushal et al., 2019). This removal

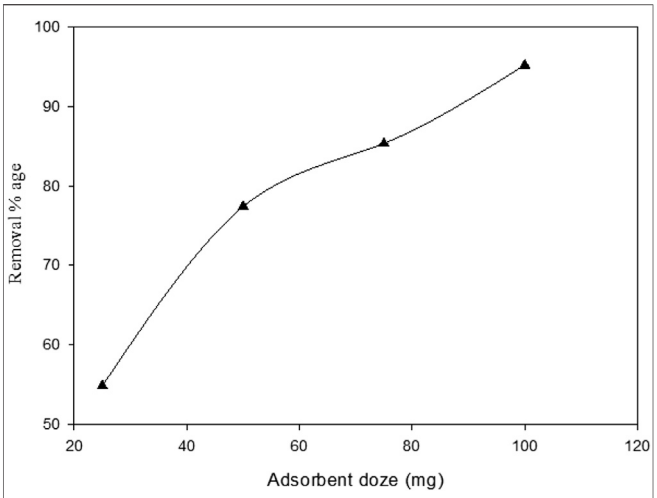

FIGURE 7 | Effect of adsorbent dose on percentage removal of phenol using Ag–WBC by sono-adsorption (Experimental conditions: phenol conc. = 10 mg L^{-1}, pH = 3, contact time = 90 min, ultrasound frequency = 35 kHz, US power= 80 W)

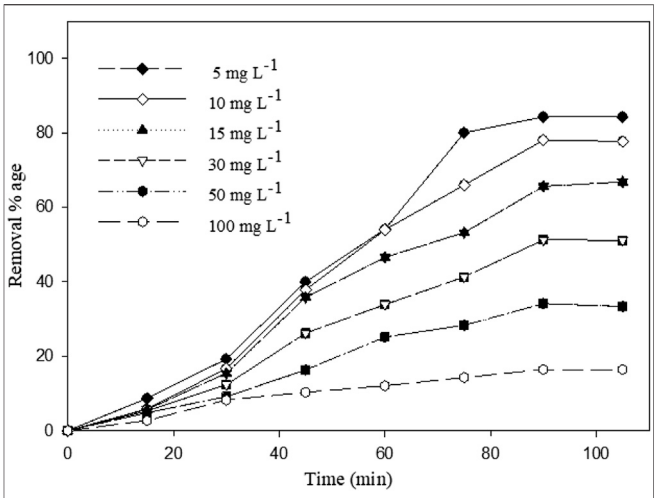

FIGURE 8 | Effect of initial phenol concentration on percentage removal of phenol using Ag–WBC by sono-adsorption (Reaction conditions: pH =3, adsorbent dose =0.05 g, US power =80 W).

explains that resulting energy from ultrasonic irradiation influences mass transfer efficacy during the convection and cavitation that is the critical phenomenon responsible for the sonochemical reaction (Midathana and Moholkar, 2009).

Effect of pH

The effect of pH was examined for the removal of phenol in the pH range from 3–9, while the initial concentration of phenol, adsorbent dosage, contact time, US power, temp, and frequency were kept constant at 10 mg L^{-1}, 0.05 g, 90 min, 80 W, 30–35°C, and 35 kHz, respectively. pH is one of the most influential parameters of adsorption studies. It influences the uptake of the adsorbate since a change in pH affects the adsorbent's surface characteristics and leads to ionization of the functional groups on the adsorbent molecule. The maximum adsorption of phenol was recorded at pH 3, as shown in **Figure 6**. However, the removal efficiency was decreased as the pH was increased to 5, 7, and 9, and a decrease was observed in percentage removal from 77 to 27%. It was found that a better phenol removal was achieved in the acidic conditions, while the increase in pH resulted in a decline in removal efficiency. Previous studies showed that a better pollutant removal was conducted under an acidic condition (Li et al., 2017). In an acidic form at pH 2–6, solid and attractive forces occurred between the adsorbent material and phenol molecule (Mohsin et al., 2013; Zhao et al., 2020). Subsequently, phenol was in the form of salt, which loses its negative charge easily and hence becomes difficult to adsorb. Moreover, the presence of OH^- ions inhibits phenol ions from being adsorbed (Afsharnia et al., 2016).

Effect of Adsorbent Dose

The study of adsorbent dosage is one of the most critical factors determining the influence of adsorbent on phenol absorption. **Figure 7** shows the effect of Ag–WBC doses on the sono-adsorption of phenol. The concentration of Ag–WBC was increased by 0.025–0.1 g, while the initial concentration of phenol, pH, contact time, US power, temp, and frequency was kept constant at 10 mg L^{-1}, pH 3, 90 min, 80 W, 30–35°C, and 35 kHz, respectively. The experimental findings indicated that the rise in the dosage led to an increase in the percentage removal of phenol from 54 to 95%. This fact can be explained from the fact that the concentration of phenol was kept constant. As a result, more available adsorption surfaces and more adsorption sites for adsorbates were found (Girish and Ramachandra Murty, 2014). In their study, the phenol removal was increased by increasing the adsorbent dosage due to the available active sites on the Ag–WBC composite, which were not saturated during the sono-adsorption process. Zhao et al., (2020) explained that the removal of phenol is directly proportional to adsorbent doses. A similar trend was found in the literature for the removal of phenol by using various materials such as sawdust (Dakhil, 2013), black tea leaves (Ali et al., 2018), tamarind seed powder (Auwal et al., 2018), and ZnO modified with Ag (Vaiano et al., 2018).

Effect of Initial Phenol Concentration in Terms of Contact Time

The effect of different initial phenol concentrations ranging 5–100 mg L^{-1} was investigated at pH 3 using 0.05 g of Ag–WBC composites for the sono-adsorptive performance of phenol (**Figure 8**) (concentration vs time). The contact time, US power, temperature, and frequency were constant at 90 min, 80 W, 30–35°C, and 35 kHz, respectively. Phenol removal percentage contributions at different initial phenol concentrations of 5, 10, 15, 30, 50, and 100 mg L^{-1} were 84.2, 78, 65.6, 51.2, 34.1, and 16.3% respectively. It was found that an increase in the initial phenol concentration led to decreases in the percentage removal efficiency due to the saturation of active adsorption sites of adsorbent. This may be justified based on the availability of more adsorption sites

TABLE 1 | Value obtained from the Langmuir and Freundlich isotherm models.

Langmuir					Freundlich			
Adsorbent	q_{exp} (mg g^{-1})	q_{max} (mg g^{-1})	K_{ads} (L_m g^{-1})	R^2	q_{exp} (mg g^{-1})	K_F (L g^{-1})	1/n	R^2
(Ag–WBC)	32.79	34.483	0.3169	0. 9,972	32.79	32.79	7.11	0.9321

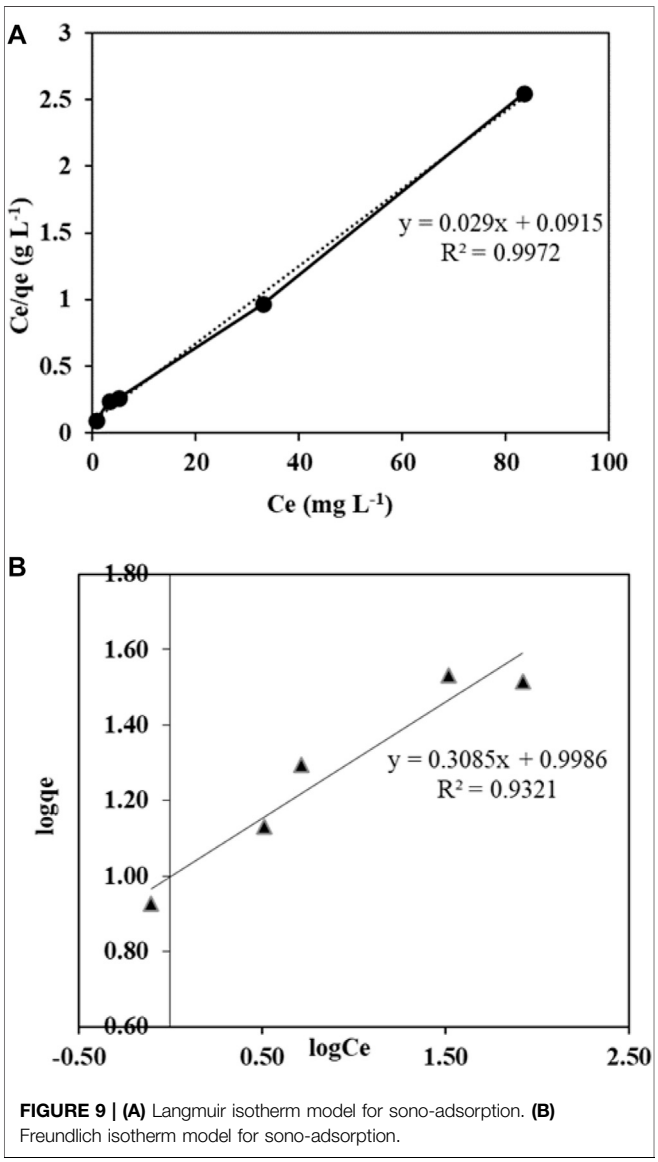

FIGURE 9 | (A) Langmuir isotherm model for sono-adsorption. **(B)** Freundlich isotherm model for sono-adsorption.

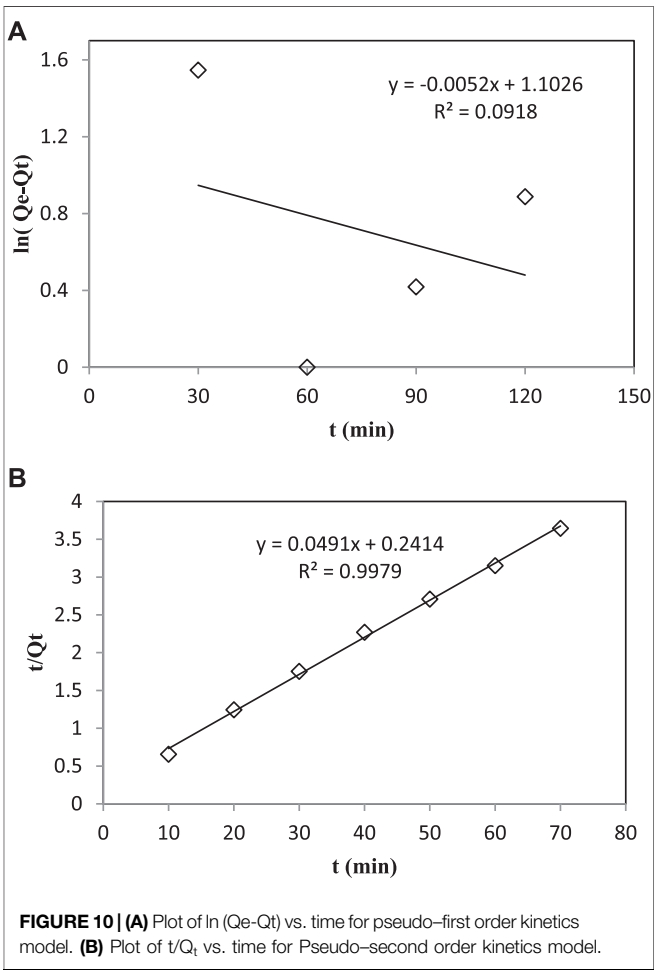

FIGURE 10 | (A) Plot of ln (Qe-Qt) vs. time for pseudo–first order kinetics model. **(B)** Plot of t/Q_t vs. time for Pseudo–second order kinetics model.

and a higher surface area of the Ag–WBC composite (Abussaud et al., 2016). The decline in phenol uptake with an increase in phenol concentration was also due to the high sono-adsorption rate at the initial phases. It gradually decreased as the time increased until attaining equilibrium. It was observed that no further increase of phenol uptake was held on rising contact time from 90 to 105 min. Hence, the contact time of 90 min was kept for sono-adsorption as the optimum time for comprehensive investigation (Abussaud et al., 2016).

Isotherm Analysis

The ultrasonic-adsorptive data was elucidated exhaustively by well-known isotherm models such as Langmuir and Freundlich (Chaudhary et al., 2013). The initial phenol concentrations 5, 10, 25, 50, and 100 mg L^{-1} were examined for the isotherm studies. At the same time, all the other parameters like US power, temp, and frequency were kept constant at 90 min, 80 W, 30–35°C, and 35 kHz, respectively. The linear forms of the functioning isotherm models and multiple isotherm parameters are shown in (**Table 1**). The plots showing the linear fitting of phenol ultrasonic-adsorptive equilibrium data with Langmuir and Freundlich isotherm models are shown in **Figures 9A,B**. The Langmuir isotherm elucidates monolayer surface adsorption, that is, in which there is homogeneous energy distribution with multilayer assumption and contaminant adsorption by the adsorbent. The Freundlich model

applies to heterogeneous surface adsorption with non-uniform distribution. This model elucidates the contaminant adsorption as multilayers on the surface of the adsorbent. It is clear from **Table 1** that the sono-adsorption process for phenol using Ag–Biochar composites is better fitted to the Langmuir isotherm (R_2 = 0.9972) as compared to Freundlich (R_2 = 0.9321), indicating monolayer adsorption on homogeneous sites of adsorbent (Kaushal et al., 2019). Similar results were reported in a previous study where modified ground-nut shell-activated carbon (MGSAC) was used as an adsorbent for phenol removal, and the adsorption was the best fit to the Langmuir isotherm. The monolayer adsorption capacity of the modified adsorbent for phenol was found at 115.5 mg/g (Eletta et al., 2020). These models were used for the determination of the maximum uptake rate in the experimentations. The Freundlich isotherm model assumes heterogeneity in the adsorption process, and that was due to the presence of different functional groups. This model was based on adsorption on heterogeneous surfaces and does not determine the maximum capacity of the adsorbent. Thus, it was applicable only at medium or low concentrations. On the other hand, the parameter 1/n value was between 0.1–1, which shows the appropriate adherence to the Langmuir isotherm model and indicates that the adsorption is favorable as in this study (Haroon et al., 2017).

Adsorption Kinetics

Adsorption kinetics is an important factor to describe the uptake rate of solute and time required for the adsorption process. In the present work, a kinetic study was performed at different time intervals for phenol adsorption by employing linear forms of pseudo-first- and second-order kinetics. Results revealed that the amount of phenol adsorbed increases with the increase in a time interval. Initially, the adsorption was more and with time it gradually decreased. This was because more active sites were available on the surface of the adsorbent initially, and therefore, adsorption occurred. But, these sites got occupied as time increased and adsorption gradually decreased (Kaushal et al., 2019).

Pseudo-First-Order Kinetics

For the pseudo-first-order kinetic model, ln ($Q_e - Q_t$) was plotted against the time interval, and the value of k was obtained from the slope of the line and Q_e from the intercept. The results showed that the value of R^2 was low indicating that the adsorption of phenol onto Ag–Biochar composites (adsorbent) does not follow pseudo-first-order kinetics (**Figure 10A**).

Pseudo-Second-Order Kinetics

For the pseudo-second-order kinetic model, data were plotted (**Eq. 7**). The results showed that the value of R^2 is high that shows the adsorption of phenol onto Ag–Biochar composites (adsorbent) following pseudo-second-order kinetics (**Figure 10B**).

CONCLUSION

In conclusion, silver-embedded wheat straw biochar composites Ag–WBC were successfully synthesized and used as a simple, green, and cost-effective way to remove phenol in an aqueous solution. The formation of silver nanoparticles obtained from *Ligustrum lucidum* leaves on the surface of wheat straw biochar was confirmed by SEM, and EDX determined elemental mapping. Ag–WBC composite modification had improved the performance of adsorption and sono-adsorption. The experimental data revealed that the maximum removal efficiency was 78% in 90 min, along with the optimization of main parameters, that is, 3 pH, 0.05 g adsorbent dose, at 10 mg L^{-1} initial concentration of phenol, 80 W ultrasonic power, 30°C temperature, and frequency of 35 kHz. The study showed that wheat straw biochar and its composites with silver had shown remarkable performance compared to biochar alone. While sono-adsorption of Ag–WBC showed superior removal ability as compared to the traditional adsorption process. On the other hand, obtained experimental results were evaluated by two well-known models, Langmuir and Freundlich. The coefficient values obtained indicate that the Langmuir model is more appropriate than the Freundlich model. The probability of the sono-adsorption process was evaluated by calculating kinetics that suggested pseudo-second-order of reaction. The proposed green approach may be used for the large-scale production of silver nanoparticles and can be used as an efficient and cost-effective method for wastewater treatment.

DATA AVAILABILITY STATEMENT

The original contributions presented in the study are included in the article/Supplementary Material; further inquiries can be directed to the corresponding author.

AUTHOR CONTRIBUTIONS

MK contributed to methodology, conducting the experiments, and writing the original draft. MS contributed to conceptualization, supervision, validation, formal analysis, and acquisition of the resources. NM contributed to review and editing. RK contributed to material acquisition, review, and editing. MB contributed to data analysis, review, and editing. NR contributed to data analysis, review, and editing. UW contributed to review and editing. IS contributed to review and editing. AA contributed to data analysis, review, and editing. MA contributed to data analysis, funding acquisition. GE-SB contributed to formal analysis and data analysis. AA-H contributed to funding acquisition, review, editing, and supervision. AK contributed to conceptualization and supervision.

ACKNOWLEDGMENTS

Authors thank Taif University supporting project TURSP 2020/91, Saudi Arabia.

REFERENCES

Abussaud, B., Asmaly, H. A., Ihsanullah, T. A., Saleh, T. A., Gupta, V. K., laoui, T., et al. (2016). Sorption of Phenol from Waters on Activated Carbon Impregnated with Iron Oxide, Aluminum Oxide and Titanium Oxide. *J. Mol. Liquids* 213, 351–359. doi:10.1016/j.molliq.2015.08.044

Afsharnia, M., Saeidi, M., Zarei, A., Narooie, M. R., and Biglari, H. (2016). Phenol Removal from Aqueous Environment by Adsorption onto Pomegranate Peel Carbon. *Electron. Physician* 8, 3248–3256. doi:10.19082/3248

Ahmed, S., SaifullahAhmad, M., Ahmad, M., Swami, B. L., and Ikram, S. (2016). Green Synthesis of Silver Nanoparticles Using Azadirachta indica Aqueous Leaf Extract. *J. Radiat. Res. Appl. Sci.* 9, 1–7. doi:10.1016/j.jrras.2015.06.006

Ali, A., Bilal, M., Khan, R., Farooq, R., and Siddique, M. (2018). Ultrasound-assisted Adsorption of Phenol from Aqueous Solution by Using Spent Black tea Leaves. *Environ. Sci. Pollut. Res.* 25 (23), 22920–22930. doi:10.1007/s11356-018-2186-9

Alnasrawy, S. T., Alkindi, G. Y., and Albayati, T. M. (2021). Removal of High Concentration Phenol from Aqueous Solutions by Electrochemical Technique. *Etj* 39, 189–195. doi:10.30684/etj.v39i2A.1705

Amina, S. J., and Guo, B. (2020). A Review on the Synthesis and Functionalization of Gold Nanoparticles as a Drug Delivery Vehicle. *Ijn* Vol. 15, 9823–9857. doi:10.2147/ijn.s279094

Arefi-Oskoui, S., Khataee, A., Safarpour, M., Orooji, Y., and Vatanpour, V. (2019). A Review on the Applications of Ultrasonic Technology in Membrane Bioreactors. *Ultrason. Sonochem.* 58, 104633. doi:10.1016/j.ultsonch.2019.104633

Ashraf, J. M., Ansari, M. A., Khan, H. M., Alzohairy, M. A., and Choi, I. (2016). Green Synthesis of Silver Nanoparticles and Characterization of Their Inhibitory Effects on AGEs Formation Using Biophysical Techniques. *Sci. Rep.* 6, 1–10. doi:10.1038/srep20414

Auwal, A., Hossen, J., and Rakib-uz-Zaman, M. (2018). Removal of Phenol from Aqueous Solution Using Tamarind Seed Powder as Adsorbent. *IOSR J. Environ. Sci. Tox. Food Technol.* 12, 41–48. doi:10.9790/2402-1203014148

Bansode, S. R., and Rathod, V. K. (2017). An Investigation of Lipase Catalysed Sonochemical Synthesis: A Review. *Ultrason. Sonochem.* 38, 503–529. doi:10.1016/j.ultsonch.2017.02.028

Biswas, B., Pandey, N., Bisht, Y., Singh, R., Kumar, J., and Bhaskar, T. (2017). Pyrolysis of Agricultural Biomass Residues: Comparative Study of Corn Cob, Wheat Straw, rice Straw and rice Husk. *Bioresour. Techn.* 237, 57–63. doi:10.1016/j.biortech.2017.02.046

Chandran, S. P., Chaudhary, M., Pasricha, R., Ahmad, A., and Sastry, M. (2006). Synthesis of Gold Nanotriangles and Silver Nanoparticles Using Aloe Vera Plant Extract. *Biotechnol. Prog.* 22, 577–583. doi:10.1021/bp0501423

Chaudhary, G. R., Saharan, P., Umar, A., Mehta, S. K., and Mor, S. (2013). Well-crystalline ZnO Nanostructures for the Removal of Acridine orange and Coomassie Brilliant Blue R-250 Hazardous Dyes. *Sci. Adv. Mat* 5, 1886–1894. doi:10.1166/sam.2013.1701

Chung, H.-K., Kim, W.-H., Park, J., Cho, J., Jeong, T.-Y., and Park, P.-K. (20152015). Application of Langmuir and Freundlich Isotherms to Predict Adsorbate Removal Efficiency or Required Amount of Adsorbent. *J. Ind. Eng. Chem.* 28, 241–246. doi:10.1016/j.jiec.2015.02.021

Cuerda-Correa, E. M., Alexandre-Franco, M. F., and Fernández-González, C. (2020). Advanced Oxidation Processes for the Removal of Antibiotics from Water. An Overview. *Water* 12, 102. doi:10.3390/w12010102

Dakhil, I. H. (2013). Removal of Phenol from Industrial Wastewater Using Sawdust. *Int. J. Eng. Sci.* 3 (1), 25–31.

Dedovic, N., Igic, S., Janic, T., Matic-Kekic, S., Ponjican., O., Tomic., M., et al. (2012). Efficiency of Small Scale Manually Fed Boilers -Mathematical Models. *Energies* 5, 1470–1489. doi:10.3390/en5051470

El-Naggar, N. E.-A., Hussein, M. H., and El-Sawah, A. A. (2017). Bio-fabrication of Silver Nanoparticles by Phycocyanin, Characterization, *In Vitro* Anticancer Activity against Breast Cancer Cell Line and *In Vivo* Cytotxicity. *Sci. Rep.* 7, 1–20. doi:10.1038/s41598-017-11121-3

Eletta, O. A. A., Tijani, I. O., and Ighalo, J. O. (2020). Adsorption of Pb (II) and Phenol from Wastewater Using Silver Nitrate Modified Activated Carbon from Groundnut (*Arachis hypogaea* L.) Shells. *W J. E* 43 (1), 26–35.Available at https://sta.uwi.edu/eng/wije/vol4301_jul2020/documents/M04_19043_v43n1p26-35_OEletta-Jul2020.pdf

Femila, E., Srimathi, R., and Deivasigamani, C. (2014). Removal of Malachite green Using Silver Nanoparticles via Adsorption and Catalytic Degradation. *Int. J. Pharm. Pharm. Sci.* 6, 579–583.

Francis, A. O., Ahmad Zaini, M. A., Muhammad, I. M., Abdulsalam, S., and El-Nafaty, U. A. (2020). Adsorption Dynamics of Dye onto Crab Shell Chitosan/neem Leaf Composite. *Int. J. Chem. React.* 15, 673–682. doi:10.2166/wpt.2020.054

Girish, C. R., and Ramachandra Murty, V. (2014). Adsorption of Phenol from Aqueous Solution Using Lantana Camara, forest Waste: Kinetics, Isotherm, and Thermodynamic Studies. *Int. Scholarly Res. Notices* 2014, 1–16. doi:10.1155/2014/201626

Hamad, H. T. (2021). Removal of Phenol and Inorganic Metals from Wastewater Using Activated Ceramic. *J. King Saud Univ. - Eng. Sci.* 33, 221–226. doi:10.1016/j.jksues.2020.04.006

Hamza, W., Dammak, N., Hadjltaief, H. B., Eloussaief, M., and Benzina, M. (2018). Sono-assisted Adsorption of Cristal Violet Dye onto Tunisian Smectite Clay: Characterization, Kinetics and Adsorption Isotherms. *Ecotoxicology Environ. Saf.* 163, 365–371. doi:10.1016/j.ecoenv.2018.07.021

Haroon, H., Gardazi, S. M. H., Butt, T. A., Pervez, A., Mahmood, Q., and Bilal, M. (2017). Novel Lignocellulosic Wastes for Comparative Adsorption of Cr(VI): Equilibrium Kinetics and Thermodynamic Studies. *Pol. J. Chem. Technol.* 19, 6–15. doi:10.1515/pjct-2017-0021

Hejazi, F., Ghoreyshi, A. A., and Rahimnejad, M. (2019). Simultaneous Phenol Removal and Electricity Generation Using a Hybrid Granular Activated Carbon Adsorption-Biodegradation Process in a Batch Recycled Tubular Microbial Fuel Cell. *Biomass and Bioenergy* 129, 105336. doi:10.1016/j.biombioe.2019.105336

Kalogianni, A. I., Lazou, T., Bossis, I., and Gelasakis, A. I. (20202020). Natural Phenolic Compounds for the Control of Oxidation, Bacterial Spoilage, and Foodborne Pathogens in Meat. *Foods* 9, 794. doi:10.3390/foods9060794

Kaushal, I., Saharan, P., Kumar, V., Sharma, A. K., and Umar, A. (2019). Superb Sono-Adsorption and Energy Storage Potential of Multifunctional Ag-Biochar Composite. *J. Alloys Compd.* 785, 240–249. doi:10.1016/j.jallcom.2019.01.064

Khan, F. U., Khan, Z. U. H., Ma, J., Khan, A. U., Sohail, M., Chen, Y., et al. (2021). An Astragalus Membranaceus Based Eco-Friendly Biomimetic Synthesis Approach of ZnO Nanoflowers with an Excellent Antibacterial, Antioxidant and Electrochemical Sensing Effect. *Mater. Sci. Eng. C* 118, 111432. doi:10.1016/j.msec.2020.111432

Kumar, N. S., Shaikh, H. M., Asif, M., and Al-Ghurabi, E. H. (2021). Engineered Biochar from wood Apple Shell Waste for High-Efficient Removal of Toxic Phenolic Compounds in Wastewater. *Sci. Rep.* 11, 2586–2602. doi:10.1007/s11356-018-2315-5

Li, H., Jiang, D., Huang, Z., He, K., Zeng, G., Chen, A., et al. (2019). Preparation of Silver-Nanoparticle-Loaded Magnetic Biochar/poly(dopamine) Composite as Catalyst for Reduction of Organic Dyes. *J. Colloid Interf. Sci.* 555, 460–469. doi:10.1016/j.jcis.2019.08.013

Li, J., Lin, H., Zhu, K., and Zhang, H. (2017). Degradation of Acid Orange 7 Using Peroxymonosulfate Catalyzed by Granulated Activated Carbon and Enhanced by Electrolysis. *Chemosphere* 188, 139–147. doi:10.1016/j.chemosphere.2017.08.137

Li, Y., Wei, J., Wang, C., and Wang, W. (2010). Comparison of Phenol Removal in Synthetic Wastewater by NF or RO Membranes. *Desalination Water Treat.* 22, 211–219. doi:10.5004/dwt.2010.1787

Liu, J., Jiang, J., Meng, Y., Aihemaiti, A., Xu, Y., Xiang, H., et al. (2020). Preparation, Environmental Application and prospect of Biochar-Supported Metal Nanoparticles: A Review. *J. Hazard. Mater.* 388, 122026. doi:10.1016/j.jhazmat.2020.122026

Liu, J., Xie, J., Ren, Z., and Zhang, W. (2013). Solvent Extraction of Phenol with Cumene from Wastewater. *Desalination Water Treat.* 51, 3826–3831. doi:10.1080/19443994.2013.796993

Mariselvam, R., Ranjitsingh, A. J. A., Usha Raja Nanthini, A., Kalirajan, K., Padmalatha, C., and Mosae Selvakumar, P. (2014). Green Synthesis of Silver Nanoparticles from the Extract of the Inflorescence of Cocos Nucifera (Family:

Arecaceae) for Enhanced Antibacterial Activity. *Spectrochimica Acta A: Mol. Biomol. Spectrosc.* 129, 537–541. doi:10.1016/j.saa.2014.03.066

Midathana, V. R., and Moholkar, V. S. (2009). Mechanistic Studies in Ultrasound-Assisted Adsorption for Removal of Aromatic Pollutants. *Ind. Eng. Chem. Res.* 48, 7368–7377. doi:10.1021/ie900049e

Mohamed, A., Yousef, S., Nasser, W. S., Osman, T., Knebel, A., Sánchez, E. P. V., et al. (2020). Rapid Photocatalytic Degradation of Phenol from Water Using Composite Nanofibers under UV. *Environ. Sci. Eur.* 32, 1–8. doi:10.1186/s12302-020-00436-0

Mohammed, N. A. S., Abu-Zurayk, R. A., Hamadneh, I., and Al-Dujaili, A. H. (2018). Phenol Adsorption on Biochar Prepared from the pine Fruit Shells: Equilibrium, Kinetic and Thermodynamics Studies. *J. Environ. Manage.* 226, 377–385. doi:10.1016/j.jenvman.2018.08.033

Mohsin, K., Anwar, R., Nadeem, F., Amir, Y., and Syed, W. (2013). Removal of Phenol from Wastewater Using Activated Waste Tea Leaves. *Pol. J. Chem. Technol.* 15 (2), 1–6. doi:10.2478/pjct-2013-0016

Mojoudi, N., Soleimani, M., Mirghaffari, N., Belver, C., and Bedia, J. (2019). Removal of Phenol and Phosphate from Aqueous Solutions Using Activated Carbons Prepared from Oily Sludge through Physical and Chemical Activation. *Water Sci. Technol.* 80, 575–586. doi:10.2166/wst.2019.305

Nanda, S., Dalai, A. K., Gökalp, I., and Kozinski, J. A. (2016). Valorization of Horse Manure through Catalytic Supercritical Water Gasification. *Waste Manag.* 52, 147–158. doi:10.1016/j.wasman.2016.03.049

Pantić, N., Prodanović, R., Đurđić, K. I., Polović, N., Spasojević, M., and Prodanović, O. (2021). Optimization of Phenol Removal with Horseradish Peroxidase Encapsulated within Tyramine-Alginate Micro-beads. *Environ. Techn. Innovation* 21, 101211. doi:10.1016/j.eti.2020.101211

Parada, H., Jr, Gammon, M. D., Ettore, H. L., Chen, J., Calafat, A. M., Neugut, A. I., et al. (2019). Urinary Concentrations of Environmental Phenols and Their Associations with Breast Cancer Incidence and Mortality Following Breast Cancer. *Environ. Int.* 130, 104890. doi:10.1016/j.envint.2019.05.084

Parthasarathy, S., Mohammed, R. R., Fong, C. M., Gomes, R. L., and Manickam, S. (2016). A Novel Hybrid Approach of Activated Carbon and Ultrasound Cavitation for the Intensification of palm Oil Mill Effluent (POME) Polishing. *J. Clean. Prod.* 112, 1218–1226. doi:10.1016/j.jclepro.2015.05.125

Peng, X., Wang, M., Hu, F., Qiu, F., Dai, H., and Cao, Z. (2019). Facile Fabrication of Hollow Biochar Carbon-Doped TiO2/CuO Composites for the Photocatalytic Degradation of Ammonia Nitrogen from Aqueous Solution. *J. Alloys Compd.* 770, 1055–1063. doi:10.1016/j.jallcom.2018.08.207

Premarathna, K. S. D., Rajapaksha, A. U., Sarkar, B., Kwon, E. E., Bhatnagar, A., Ok, Y. S., et al. (2019). Biochar-based Engineered Composites for Sorptive Decontamination of Water: A Review. *Chem. Eng. J.* 372, 536–550. doi:10.1016/j.cej.2019.04.097

Rene, E. R., Shu, L., Lens, P. N. L., and Jegatheesan, J. V. (2018). Tools, Techniques, and Technologies for Pollution Prevention, Control, and Resource Recovery. *Environ. Sci. Pollut. Res.* 25, 5047–5050. doi:10.1007/s11356-018-1319-5

Restrepo, C. V., and Villa, C. C. (2021). Synthesis of Silver Nanoparticles, Influence of Capping Agents, and Dependence on Size and Shape: A Review. *Environ. Nanotechnol. Monit. Manag.* 15, 100428. doi:10.1016/j.enmm.2021.100428

Saad, M., Tahir, H., and Ali, D. (2017). Green Synthesis of Ag-Cr-AC Nanocomposites by Azadirachta indica and its Application for the Simultaneous Removal of Binary Mixture of Dyes by Ultrasonicated Assisted Adsorption Process Using Response Surface Methodology. *Ultrason. Sonochem.* 38, 197–213. doi:10.1016/j.ultsonch.2017.03.022

Saleh, M. E., Mahmoud, A. H., and Rashad, M. (2013). "Biochar Usage as a Cost-Effective Bio-Sorbent for Removing NH4-N from Wastewater," in The international conference the Global Climate Change, Biodiversity and Sustainability: Challenges and Opportunities in Arab MENA region and EuroMed, Alexandria, Egypt, 15-18 April 2013 (Arab Academy for Science, Technology and Maritime Transport, Smithsonian Conservation Biology Institute, and the University of Prince Edward Island), 15–18.

Santhosh, C., Daneshvar, E., Tripathi, K. M., Baltrėnas, P., Kim, T., Baltrėnaitė, E., et al. (2020). Synthesis and Characterization of Magnetic Biochar Adsorbents for the Removal of Cr(VI) and Acid orange 7 Dye from Aqueous Solution. *Environ. Sci. Pollut. Res.* 27, 32874–32887. doi:10.1007/s11356-020-09275-1

Sharma, S., Sharma, S., and Vig, A. P. (2018). Antigenotoxic Potential of Plant Leaf Extracts of *Parkinsonia aculeata* L. Using Allium cepa Assay. *Plant Physiol. Biochem.* 130, 314–323. doi:10.1016/j.plaphy.2018.07.017

Siddique, M., Farooq, R., and Price, G. J. (2014). Synergistic Effects of Combining Ultrasound with the Fenton Process in the Degradation of Reactive Blue 19. *Ultrason. Sonochem.* 21, 1206–1212. doi:10.1016/j.ultsonch.2013.12.016

Singh, P., Sarswat, A., Pittman, C. U., Mlsna, T., Jr., and Mohan, D. (2020). Sustainable Low-Concentration Arsenite [As(III)] Removal in Single and Multicomponent Systems Using Hybrid Iron Oxide-Biochar Nanocomposite Adsorbents-A Mechanistic Study. *ACS Omega* 5 (6), 2575–2593. doi:10.1021/acsomega.9b02842

Thang, P. Q., Jitae, K., Giang, B. L., Viet, N. M., and Huong, P. T. (2019). Potential Application of Chicken Manure Biochar towards Toxic Phenol and 2,4-dinitrophenol in Wastewaters. *J. Environ. Manage.* 251, 109556. doi:10.1016/j.jenvman.2019.109556

Tomei, M. C., Angelucci, D. M., Clagnan, E., and Brusetti, L. (2021). Anaerobic Biodegradation of Phenol in Wastewater Treatment: Achievements and Limits. *Appl. Microbiol. Biotechnol.* 1–30. doi:10.1007/s00253-021-11182-5

Vaiano, V., Matarangolo, M., Murcia, J. J., Rojas, H., Navío, J. A., and Hidalgo, M. C. (2018). Enhanced Photocatalytic Removal of Phenol from Aqueous Solutions Using ZnO Modified with Ag. *Appl. Catal. B: Environ.* 225, 197–206. doi:10.1016/j.apcatb.2017.11.075

Veisi, H., Azizi, S., and Mohammadi, P. (2018). Green Synthesis of the Silver Nanoparticles Mediated by Thymbra Spicata Extract and its Application as a Heterogeneous and Recyclable Nanocatalyst for Catalytic Reduction of a Variety of Dyes in Water. *J. Clean. Prod.* 170, 1536–1543. doi:10.1016/J.JCLEPRO.2017.09.265

Villegas, L. G. C., Mashhadi, N., Chen, M., Mukherjee, D., Taylor, K. E., and Biswas, N. (2016). A Short Review of Techniques for Phenol Removal from Wastewater. *Curr. Pollut. Rep* 2, 157–167. doi:10.1007/s40726-016-0035-3

Wang, L., Ok, Y. S., Tsang, D. C. W., Alessi, D. S., Rinklebe, J., Wang, H., et al. (2020). New Trends in Biochar Pyrolysis and Modification Strategies: Feedstock, Pyrolysis Conditions, Sustainability Concerns and Implications for Soil Amendment. *Soil Use Manage* 36, 358–386. doi:10.1111/sum.12592

Wang, Y., Arandiyan, H., Scott, J., Bagheri, A., Dai, H., and Amal, R. (2017). Recent Advances in Ordered Meso/macroporous Metal Oxides for Heterogeneous Catalysis: a Review. *J. Mater. Chem. A.* 5, 8825–8846. doi:10.1039/c6ta10896b

Yadav, L. S., Mishra, B. K., and Kumar, A. (2019). Adsorption of Phenol from Aqueous Solutions by Bael Furit Shell Activated Carbon: Kinetic, Equilibrium, and Mass Transfer Studies. *Theor. Found. Chem. Eng.* 53, 122–131. doi:10.1134/S0040579519010184

Yavuz, Y., and Koparal, A. (2006). Electrochemical Oxidation of Phenol in a Parallel Plate Reactor Using Ruthenium Mixed Metal Oxide Electrode. *J. Hazard. Mater.* 136, 296–302. doi:10.1016/j.jhazmat.2005.12.018

Yin, Z., Liu, Y., Liu, S., Jiang, L., Tan, X., Zeng, G., et al. (2018). Activated Magnetic Biochar by One-step Synthesis: Enhanced Adsorption and Coadsorption for 17β-Estradiol and Copper. *Sci. Total Environ.* 639, 1530–1542. doi:10.1016/j.scitotenv.2018.05.130

Younis, A. M., Elkady, E. M., and Saleh, S. M. (2020). Novel Eco-Friendly Amino-Modified Nanoparticles for Phenol Removal from Aqueous Solution. *Environ. Sci. Pollut. Res.* 27, 30694–30705. doi:10.1007/s11356-020-09313-y

Zarin, S., Aslam, Z., Zahir, A., Kamal, M. S., Rana, A. G., Ahmad, W., et al. (2018). Synthesis of Bimetallic/carbon Nanocomposite and its Application for Phenol Removal. *J. Iran. Chem. Soc.* 15, 2689–2701. doi:10.1007/s13738-018-1457-1

Zhang, B., Zhou, S., Zhou, L., Wen, J., and Yuan, Y. (2019). Pyrolysis Temperature-dependent Electron Transfer Capacities of Dissolved Organic Matters Derived from Wheat Straw Biochar. *Sci. Total Environ.* 696, 133895. doi:10.1016/j.scitotenv.2019.133895

Zhao, C., Zhong, S., Li, C., Zhou, H., and Zhang, S. (2020). Property and Mechanism of Phenol Degradation by Biochar Activated Persulfate. *J. Mater. Res. Techn.* 9, 601–609. doi:10.1016/j.jmrt.2019.10.089

Zhou, J., Chen, H., Huang, W., Arocena, J. M., and Ge, S. (2016). Sorption of Atrazine, 17α-Estradiol, and Phenanthrene on Wheat Straw and Peanut Shell Biochars. *Water Air Soil Pollut.* 227, 1–13. doi:10.1007/s11270-015-2699-5

Zia, M., Gul, S., Akhtar, J., Haq, I. U., Abbasi, B. H., and Hussain, A. (2017). Green Synthesis of Silver Nanoparticles from Grape and Tomato Juices and Evaluation of Biological Activities. *IET Nanobiotechnol.* 11, 193–199. doi:10.1049/iet-nbt.2015.0099

Conflict of Interest: The authors declare that the research was conducted in the absence of any commercial or financial relationships that could be construed as a potential conflict of interest.

Publisher's Note: All claims expressed in this article are solely those of the authors and do not necessarily represent those of their affiliated organizations, or those of the publisher, the editors, and the reviewers. Any product that may be evaluated in this article, or claim that may be made by its manufacturer, is not guaranteed or endorsed by the publisher.